Electronic supplementary information for

# Concurrent conductance and transition voltage spectroscopy study of scanning tunneling microscopy vacuum junctions. Does it unravel new physics?

**Ioan Bâldea** * [a‡]

## S1 Tunneling current

The tunneling electron current per unit area $I$ along the $z$-direction across an energy barrier placed between two (STM-tip and substrate) electrodes under bias $V$ ($\mu_t - \mu_s = eV > 0$) having infinite transverse $(x,y)$ extension can be expressed as [1,2]

$$I_{tunnel} = K\left[eV\int_{-E_F}^{\mu_s}\mathscr{T}(E_z;V)dE_z - \int_{\mu_s}^{\mu_t}E_z\mathscr{T}(E_z;V)dE_z\right]. \tag{S1}$$

Once the barrier potential is known [eqn (1)], the transmission coefficient $\mathscr{T}$ can be obtained exactly by numerically solving the Schrödinger equation.[3]. The numerical factor entering eqn (5) can be easily obtained by using the value of the prefactor

$$K = 4\pi emh^{-3} = 1.618\times 10^8\,\mathrm{pA\,nm^{-2}\,eV^{-2}}, \tag{S2}$$

where $m$ and $-e$ stand for electron mass and charge, respectively.

Although we have used eqn (S1) for all numerical results presented in the main text, we mention that results obtained by assuming a highly lateral constriction[2,4] (one-channel Landauer formula)

$$I_{tunnel} \propto \int_{\mu_s}^{\mu_t}\mathscr{T}(E_z;V)dE_z \tag{S3}$$

are qualitatively similar and do not alter the conclusions of this work.

## S2 Effects relevant for a realistic rarrier

Fig. S1 and Fig. S2 demonstrate that attempts to make the tunneling barrier more realistic do not improve the agreement between theory and experiment: $V_t$ continues to increase roughly linear with $1/d$, and $G$ exhibits an overall exponential decay with increasing $d$. To show that the potential profile has no substantial impact on $V_t$, we present in Fig. S1a results for two extreme situations. The linear potential drop of eqn (2) is one extreme idealization. The other extreme idealization would be a flat potential [$z$-independent $V_b$ in eqn (1)]. Fig. S1b and Fig. S1c show that considering rather broad distributions of nanogap sizes and work functions rather than sharp $d$ and $\Phi$'s do not improve the agreement with experiment.

## S3 Ghost transmission

Adding a small contribution $\tau$ [given in the legend of Fig. S3) to the transmission by tunneling ($\mathscr{T} \to \mathscr{T} + \tau$ in the RHS of eqn (S1] — which could mimics an extra contribution due to pseudo-diffusion or hopping has an effect similar to the ghost current. This is visible by comparing Fig. S3 shown below with Fig. 3 of the main text.

## S4 The activation energy: an important issue for charge hopping

To make clear that fact that the large activation energies extracted from the experimental data[7,8] represent an important issue for assigning the charge transport in longer molecules as *entirely* due to hopping, we briefly expose the main difficulty, closely following ref. 7.

Within Marcus' electron transfer theory, the activation energy $E_a$ that determines the Arrhenius temperature ($T$) dependence of the conductance

$$G \propto \exp\left(-E_a/k_BT\right), \tag{S4}$$

where $k_B$ is Boltzmann's constant, can be expressed in terms of the thermodynamic driving force $\Delta F$ and the reorganization energy $\lambda$ [7]

$$E_a = \frac{(\lambda+\Delta F)^2}{4\lambda} \simeq \frac{\lambda}{4}. \tag{S5}$$

[a] *Theoretische Chemie, Universität Heidelberg, Im Neuenheimer Feld 229, D-69120 Heidelberg, Germany.*
‡ E-mail: ioan.baldea@pci.uni-heidelberg.de. Also at National Institute for Lasers, Plasmas, and Radiation Physics, Institute of Space Sciences, Bucharest, Romania

The above approximation is justified by the smallness of the driving force $\Delta F (\ll \lambda)$; typical values are a few tens of meV for $\Delta F$ and a few tenths of eV for $\lambda$. $\Delta F$ is basically given by the variation in hopping site energies related to the potential drop across the junction. For CP-AFM junctions, the above reorganization energy entering eqn (S5) comprises the contributions of intramolecular reorganization ($\lambda_i$) and of environmental reorganization ($\lambda_o$)

$$\lambda = \lambda_o + \lambda_i \approx 2\lambda_i. \tag{S6}$$

$\lambda_o$ embodies polarization effects of $\sim 100$ molecules that form a CP-AFM junction. As done above, a common procedure is to assume

$$\lambda_o \approx \lambda_i \tag{S7}$$

and to estimate the intramolecular reorganization $\lambda_i$ by means of DFT calculations[7]. For the longer molecular species that exhibit thermally activated conduction, calculations at DFT/M062X/6-61G** level yielded values $\lambda_i = 0.30 - 0.10$ eV for the ONI series (*cf.* Table S4 of ref. 7) and $\lambda_i = 0.41 - 0.17$ eV for the OPI series (*cf.* Table S6 of ref. 7). When using the B3LYP functional instead of M062X, values smaller by a factor of at least 2 were found (*cf.* Tables S5 and S7 of ref. 7). Even if the larger M062X-based $\lambda_i$-values are used, by comparing the activation energies deduced from eqn (S5) and (S6) with the experimental values ($E_a \approx 0.54 - 0.62$ eV for ONI's[7] and $E_a \approx 0.28$ eV for OPI's[9]) one has to conclude that the mismatch amounts to a factor of at least $2-3$.

Although this is already quite important in view of the exponential dependence of eqn (S4) one should still note that the above $\lambda_i$ should represent drastic overestimations: they embody the contributions of *all* intramolecular vibrations, while one should merely consider the contributions of very low frequency modes, which are the only ones can be thermally activated[10].

## Notes and references


1 A. Sommerfeld and H. Bethe, *Handbuch der Physik*, Julius-Springer-Verlag, Berlin, 1933, vol. 24 (2), p. 446.
2 I. Bâldea and H. Köppel, *Phys. Stat. Solidi (b)*, 2012, **249**, 1791–1804.
3 I. Bâldea and H. Köppel, *Phys. Lett. A*, 2012, **376**, 1472 – 1476.
4 I. Bâldea, *Europhys. Lett.*, 2012, **98**, 17010.
5 I. Bâldea, *J. Phys. Chem. Solids*, 2012, **73**, 1151 – 1153.
6 I. Bâldea, *Nanoscale*, 2013, **5**, 9222–9230.
7 S. H. Choi, C. Risko, M. C. R. Delgado, B. Kim, J.-L. Bredas and C. D. Frisbie, *J. Amer Chem. Soc.*, 2010, **132**, 4358 – 4368.
8 T. Hines, I. Diez-Perez, J. Hihath, H. Liu, Z.-S. Wang, J. Zhao, G. Zhou, K. Müllen and N. Tao, *J. Am. Chem. Soc.*, 2010, **132**, 11658–11664.
9 S. H. Choi, B. Kim and C. D. Frisbie, *Science*, 2008, **320**, 1482–1486.
10 I. Bâldea, *J. Phys. Chem. C*, 2014, **118**, 8676–8684.


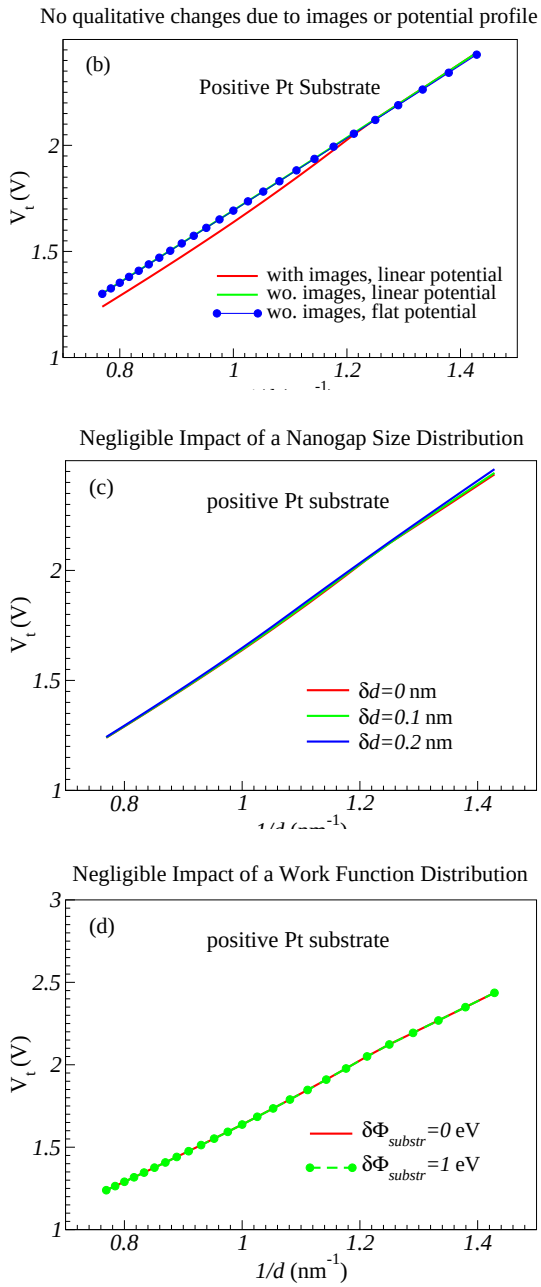


**Fig. S1** Transition voltage $V_t$ as a function of the inverse nanogap size $d$ for STM-tip of tungsten ($\Phi_W = 4.55$ eV) and substrates of Pt ($\Phi_{Pt} = 5.65$ eV) and Au ($\Phi_{Au} = 5.2$ eV). Neither (a) ignoring image charges nor the potential profile, neither a uniform distribution of (b) $d$ nor (c) of Pt-substrate work function $W$ having finite widths denoted by $\delta\ldots$ and indicated in the legend qualitatively affects the approximate linear increase $V_t \propto 1/d$ .

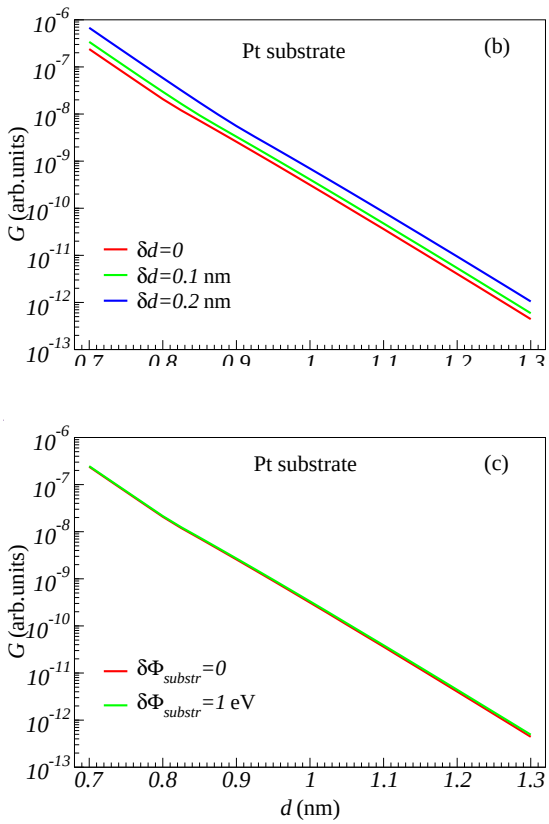


**Fig. S2** Ohmic conductance $G$ as a function of the nanogap size $d$ for STM-tip of tungsten ($\Phi_W = 4.55$ eV) and substrates of Pt ($\Phi_{Pt} = 5.65$ eV) and Au ($\Phi_{Au} = 5.2$ eV). Neither a uniform distribution of (a) $d$ nor (b) of Pt-substrate work function $W$ having finite widths denoted by $\delta\ldots$ and indicated in the legend qualitatively affects the almost exponential decay.

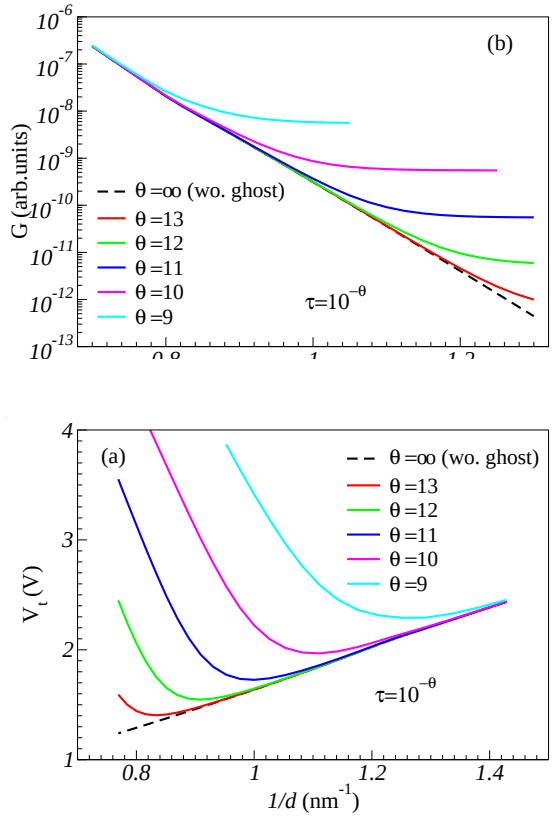


**Fig. S3** (a) Transition voltage $V_t$ and (b) Ohmic conductance $G$ as a function of the nanogap size $d$ for STM-tip of tungsten ($\Phi_W = 4.55$ eV) and substrates of Pt at positive biases ($\Phi_{Pt} = 5.65$ eV) in the presence of a ghost channel of dimensionless resistivity $\overline{\rho} = 10^{\nu}$. $\nu$-values are given in the legend. Image charge effects are included using the exact classical interaction[2,4,5], which is cutoff close to electrodes using the procedure described elsewhere[6].